IECAG 2021

Proceedings

Classification of Hyperspectral Images with CNN in Agricultural Lands †

Eren Can Seyrek *and Murat Uysal

[1] Department of Geomatics Engineering, Afyon Kocatepe University, 03200 Afyonkarahisar, Turkey
[2] Remote Sensing and GIS Research and Application Center, Afyon Kocatepe University, 03200 Afyonkarahisar, Turkey
* Correspondence: ecseyrek@aku.edu.tr
† Presented at the 1st International Electronic Conference on Agronomy, 3–17 May 2021; Available online: https://sciforum.net/conference/IECAG2021

Abstract: Hyperspectral images (HSI) offer detailed spectral reflectance information about sensed objects under favour of hundreds of narrow spectral bands. HSI have a leading role on a broad range of applications, such as forestry, agriculture, geology and environmental sciences. Monitoring and managing of agricultural lands has a great importance on meeting nutritional and other needs of rapidly and continuously increasing world's population. In this case, classification of HSI is an effective way to creating land use and land cover maps fast and accurately. In recent years, classifying of HSI with convolutional neural networks (CNN) which is a sub-field of deep learning become a very popular research topic and several CNN architectures were developed by researchers. The aim of this study is to investigate the classification performance of CNN model on agricultural HSI scenes. For this purpose, a 3D-2D CNN framework and well-known support vector machine (SVM) model were compared by using Indian Pines and Salinas Scene datasets that contain crop and mixed vegetation classes. As a result of this study, using of 3D-2D CNN has a superior performance on classifying agricultural HSI datasets.

Keywords: hyperspectral images (HSI); image classification; convolutional neural networks (CNN); support vector machine (SVM)

Citation: Lastname, F.; Lastname, F.; Lastname, F. Title. *Proceedings* **2021**, *68*, x. https://doi.org/10.3390/xxxxx

Published: date

1. Introduction

Remote sensing data obtained from airborne and spaceborne sensors are become provide more detailed spatial and spectral resolution with the developments in recent years. Through these improvements, remotely sensed data is a time-saving and low-cost alternative to precision agriculture and forestry applications. In particular, applications like detecting and separating various vegetation species, determining the conditions of crops require a rich spectral and spatial resolution. Hyperspectral images (HSI) are the most suitable data for the aforementioned analyses, by providing high spectral resolution with hundreds of spectral bands. Many studies in the literature were performed to produce highly accurate classification maps and identify land cover types by classifying HSIs. However, high spectral information reveals a huge volume of data and high dimensionality. This causes Hughes phenomenon which is one of main problems in HSI classification problems [1]. Traditional classifiers such as Maximum Likelihood and Spectral Angle Mapper cannot handle HSI data with high classification accuracy due to these problems.

In the last three decades, various studies have been conducted to apply the high classification success of Machine Learning (ML) methods to HSI classification problems. Gualtieri et al. [2] applied the SVM model with ad-hoc kernel to Indian Pines (IP) and

Salinas Scene (SS) data sets and gained 87.3% and 98.6% overall accuracy (OA) respectively. Chan & Paelinckx [3] compared tree-based Random Forest and Adaboost algorithms on a HSI obtained with HyMap sensor. The result of this study showed that Adaboost showed slightly better OA while Random Forest requires less processing time. In recent years, Convolutional Neural Network (CNN) algorithms that have become more widespread on various application fields, has been used in the HSI classification. Luo et al. [4] proposed HSI-CNN and HSI-CNN+XGBoost architectures to HSI data sets. Experimental results with common HSI benchmark data sets showed that proposed methods provided more than 99% of OA. Roy et al. [5] proposed the HybridSN architecture that both spatial-spectral and spatial feature extraction capability from HSIs. The architecture provides over 99% of OA on various benchmark data sets. Nevertheless, the HyRANK data set hardly ever used as a benchmark in studies in the literature despite IP and SS datasets are commonly used in studies.

In this study, classification performance of SVM and CNN algorithms were evaluated. For this purpose, two publicly available HSI data sets, namely SS and HyRANK Loukia (HL), were used. The data sets contain various land classes related to agriculture and forestry. In the data preparation stage, Principal Component Analysis (PCA) was applied to both data sets to reduce band numbers and avoid high dimensionality of HSI. There are 150 training samples were selected almost every class from both data sets to simulate a limited train sample scenario. After performing the classification models into HSIs, classification performances of the algorithms were evaluated by examining OA, producer accuracy (PA), user accuracy (UA), f scores, and kappa coefficient (κ) respectively.

2. Classification Methods

2.1. Support Vector Machines (SVM)

SVM is a supervised and non-parametric ML algorithm based on statistical learning theory, developed by Vapnik [6]. There are no assumptions about data distribution. In binary classification problems that classes can be separated linearly, classes can be separate with infinite number of linear decision boundaries. The main approach of SVM is to find the best decision boundary that minimizes generalization error, called as optimum hyperplane [7, 8]. Data samples that are closest to the hyperplane were used to measure the margin, called as support vectors (SV) [7]. Because of considering only SVs, SVM can be useful with limited training sets, where collecting training data is costly in terms of both time and resources [9, 10]. In most classification problems, such as remotely sensed images, classes cannot be separated by linear hyperplanes. To overcome of this situation, kernel functions are used to transform the to a larger feature space. Commonly used kernels are linear, sigmoid, polynomial, and radial basis function (RBF) [11]. However, the RBF kernel outperforms on most classification problems [11, 12]. Therefore, the RBF was used in this study when implementing the SVM model, by determining C and γ parameters with the grid search algorithm.

2.2. Convolutional Neural Networks (CNNs)

CNN is a form of deep learning that processes data in the form of multiple arrays such as, 1- dimensional data including sequences and signals, 2-dimensional data including images and audio spectrograms, 3-dimensional data including volumetric images and videos [13]. CNNs are generally formed of three fundamental components with serves different purposes, named as convolution layer, pooling layer and fully connected layer. In the convolution layer, various kernels are utilized the entire input data (tensors) and feature maps are created [14]. Subsequently, feature maps put into an activation function to generate output feature maps, such as ReLU. A pooling layer is applied the convolution layers in most CNN models in order to reduce the dimensionality of output feature maps. Third and last type of layer is the fully connected layer, where neurons are fully connected to all neurons in the previous layer, as in a regular artificial neural network [15]. Following that, this layer is connected to a classifier, such as Softmax, and classification is performed.

In this study, a hybrid CNN model is used to classify HSIs which can be able to extract spectral and spatial features along bands using 3D and 2D convolution operations. To avoid spectral redundancy of HSI, PCA transformation is applied along bands and the first 15 principal components are used. The model contains two 3D convolution layers and one 2D convolution layer respectively. The 2D convolution operation can extract only spatial features of input data. In the 3D convolution operation, spectral and spatial learning is performed simultaneously. PReLU activation function is selected for its advantages over ReLU [16]. All weights are randomly initialized and trained using back-propagation algorithm with the Adam optimizer by using the softmax classifier. Epoch and batch size parameters are detected as 256 and 500 respectively. The summary of CNN model is given at Table 1.

Table 1. Summary of the CNN model.

Layer	Type	SS data set		HL data set	
		Output shape	**# of learnable parameters**	**Output shape**	**# of learnable parameters**
1	Input	(None,7,7,15,1)	0	(None,7,7,15,1)	0
2	3D convolution	(None,5,5,9,8)	2 312	(None,5,5,9,8)	2 312
3	3D convolution	(None,3,3,5,16)	6 496	(None,3,3,5,16)	6 496
4	Reshape	(None,3,3,80)	0	(None,3,3,80)	0
5	2D convolution	(None,1,1,64)	46 208	(None,1,1,64)	46 208
6	Flatten	(None,64)	0	(None,64)	0
7	Dense	(None,256)	16 896	(None,256)	16 896
8	Dropout (40%)	(None,256)	0	(None,256)	0
9	Dense	(None,128)	33 024	(None,128)	33 024
10	Dropout (40%)	(None,128)	0	(None,128)	0
11	Dense	(None,16)	2 064	(None,14)	1806
Total number of learnable parameters:			107 000		106 742

3. Experiments

3.1. Dataset Description

SS data was acquired on 9th October by AVIRIS sensor with a 3.7-meter spatial resolution and 224 bands. To train the algorithms, 150 samples were selected randomly from each class. Numbers of training and testing samples were given in Table 2. Final size of hypercube is 512×217×204. The image composition and ground truth of SS were given in Figure 1.

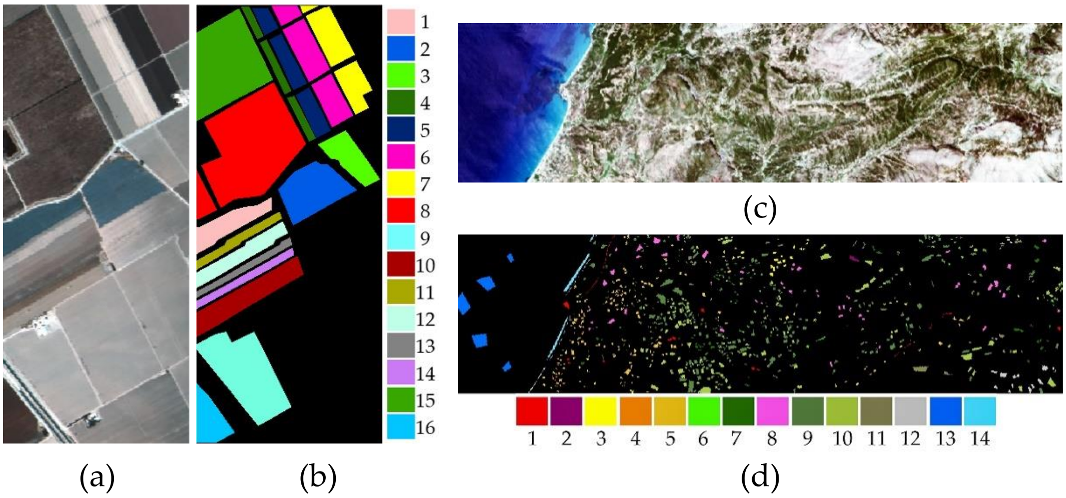

Figure 1. True color and labeled views of HSIs: (a) RGB composite and (b) ground truth of the SS with legend, and (c) RGB composite and (d) ground truth of the HL.

HyRANK data set is developed by scientific initiative of the ISPRS, WG III/4 [17]. The data was obtained from EO-1 Hyperion sensor with 30 m spatial resolution and 220 bands. Only the Loukia (HL) data was considered in this study, while HyRANK contains 5 HSI data. Ground Truth of HL contains 14 ground classes. The size of HL is 250×1376×176. The image composition and ground truth of HL was given in Figure 1. Since the 2nd and 4th classes have limited samples on the HL, 150 samples were chosen randomly from all classes except the aforementioned classes equally to train the algorithms. There are 30 samples were chosen from 2nd and 4th classes. Numbers of training and testing samples for HL were given in Table 2.

Table 2. Number of samples of the SS and HL datasets.

	SS data set			**HL data set**		
#	**Class Name**	**Train**	**Test**	**Class Name**	**Train**	**Test**
1	Brocoli_green_weeds_1	150	1859	Dense urban fabric	150	138
2	Brocoli_green_weeds_2	150	3576	Mineral extraction sites	30	37
3	Fallow	150	1826	Non irrigated arable land	150	392
4	Fallow_rough_plow	150	1244	Fruit trees	30	49
5	Fallow_smooth	150	2528	Olive groves	150	1251
6	Stubble	150	3809	Broad leaved forest	150	73
7	Celery	150	3429	Coniferous forest	150	350
8	Grapes_untrained	150	11121	Mixed forest	150	922
9	Soil_vinyard_develop	150	6053	Dense sclerophyllous vegetation	150	3643
10	Corn_senesced_green_weeds	150	3128	Sparce sclerophyllous vegetation	150	2653
11	Lettuce_romaine_4wk	150	918	Sparsely vegetated areas	150	254
12	Lettuce_romaine_5wk	150	1777	Rocks and sand	150	337
13	Lettuce_romaine_6wk	150	766	Water	150	1243

14	Lettuce_romaine_7wk	150	920	Coastal water	150	301
15	Vinyard_untrained	150	7118			
16	Vinyard_vertical_trellis	150	1657			

3.2. Experimental Results

The classification models were built by using Python's Tensorflow [18] and Scikit-learn [19] libraries. The best C and γ parameters were determined for both datasets as 100 and 0.1 respectively with grid search. To compare the classification performances of the algorithms, OA, PA, UA, f scores, and κ were calculated. Accuracy metrics for data sets were given in Table 3. As can be seen from OA and κ accuracy metrics in the table, the CNN outperformed against SVM on both data sets. For the SS data set, the CNN showed slightly better performance from SVM on 3rd, 4th, 5th, and 10th classes. Yet, the CNN's PA, UA and f score values for the 8th and 15th classes are significantly higher than SVM's. The SVM only showed slightly better performance according to PA on 16th class, where is 0.01 higher than CNN's. When comparing processing times, it is clear that CNN is faster because the SVM parameter tuning process is included in the training time.

Figure 2.a and Figure 2.b shows the classification maps for SS data set. Some pixels of the parcel on the upper-left of the image labeled as Fallow_rough_plow class on the ground truth data were misclassified by both classification algorithms. Other considerable misclassification is, upper-right parcel where was classified as Vinyard_vertical_trellis by CNN was classified by SVM as Lettuce_romaine_6wk and Vinyard_vertical_trellis, where has any ground truth data.

For the HL data set, the CNN showed better classification performance in almost every class by evaluating OA and κ metrics. In 2nd, 10th, and 15th classes, SVM's PA values are slightly higher than CNN's PA' values. Also, 12th class showed better classification performance on the SVM. PA of 1st, 6th, and 7th classes obtained a low value in the range from 0.16 to 0.62 for both classification algorithms, indicating that classification performance is considerably worse than other classes. Reason of misclassification of the aforementioned classes could be that boundary limits for these classes on feature space cannot be defined properly. Moreover, low spatial resolution of the spaceborne HSI causes mixed pixel problem. Considering the training time of the algorithms, the SVM was outperformed against CNN.

Figure 2.c and Figure 2.d shows the classification maps for HL data set. It can be seen from Figure 2.d that some pixels are misclassified on the sea along the line where Coastal water and Water classes were jointed. On the other hand, visually analysis of the result is harder than the other data set since the ground data was not collected with larger region of interests from wide areas.

Table 3. The performance analysis of classification algorithms.

Class ID	SS data set						HL data set					
	SVM			CNN			SVM			CNN		
	PA	UA	f score	PA	UA	f score	PA	UA	f score	PA	UA	f score
1	1.00	1.00	1.00	1.00	1.00	1.00	0.47	0.88	0.61	**0.62**	**0.97**	**0.76**
2	1.00	1.00	1.00	1.00	1.00	1.00	**1.00**	0.84	0.91	0.97	**1.00**	**0.99**
3	0.97	0.98	0.98	**0.99**	**1.00**	**0.99**	0.79	0.88	0.83	**0.85**	**0.91**	**0.88**
4	0.98	0.99	0.99	**0.99**	**1.00**	0.99	0.70	0.57	0.63	**0.79**	**0.86**	**0.82**
5	0.98	0.98	0.98	**0.99**	**0.99**	**0.99**	0.92	0.89	0.90	**0.97**	**0.93**	**0.95**
6	1.00	1.00	1.00	1.00	1.00	1.00	0.16	0.82	0.27	**0.20**	**0.99**	**0.34**
7	1.00	1.00	1.00	1.00	1.00	1.00	0.45	0.84	0.59	**0.56**	**0.86**	**0.68**
8	0.83	0.79	0.81	**0.92**	**0.88**	**0.90**	0.49	0.69	0.58	**0.70**	**0.83**	**0.75**
9	1.00	1.00	1.00	1.00	1.00	1.00	0.83	0.56	0.67	**0.85**	**0.64**	**0.73**
10	0.96	0.97	0.97	**0.97**	**0.99**	**0.98**	**0.80**	0.80	0.80	0.79	**0.81**	0.80

11	0.94	0.99	0.97	0.99	1.00	1.00	0.67	0.96	0.79	**0.81**	**0.99**	**0.89**
12	0.99	1.00	0.99	1.00	1.00	1.00	**0.88**	0.95	**0.92**	0.83	**0.96**	0.89
13	0.99	0.99	0.99	1.00	1.00	1.00	1.00	1.00	1.00	1.00	1.00	1.00
14	0.96	0.99	0.97	0.99	1.00	0.99	**1.00**	1.00	1.00	0.99	1.00	1.00
15	0.70	0.74	0.72	**0.84**	**0.88**	**0.86**						
16	**0.99**	1.00	0.99	0.98	1.00	0.99						
OA		91.36			**95.68**			76.37			**81.38**	
κ		90.36			**95.17**			72.05			**77.77**	
time (s)		31.72			**28.85**			**21.10**			23.16	

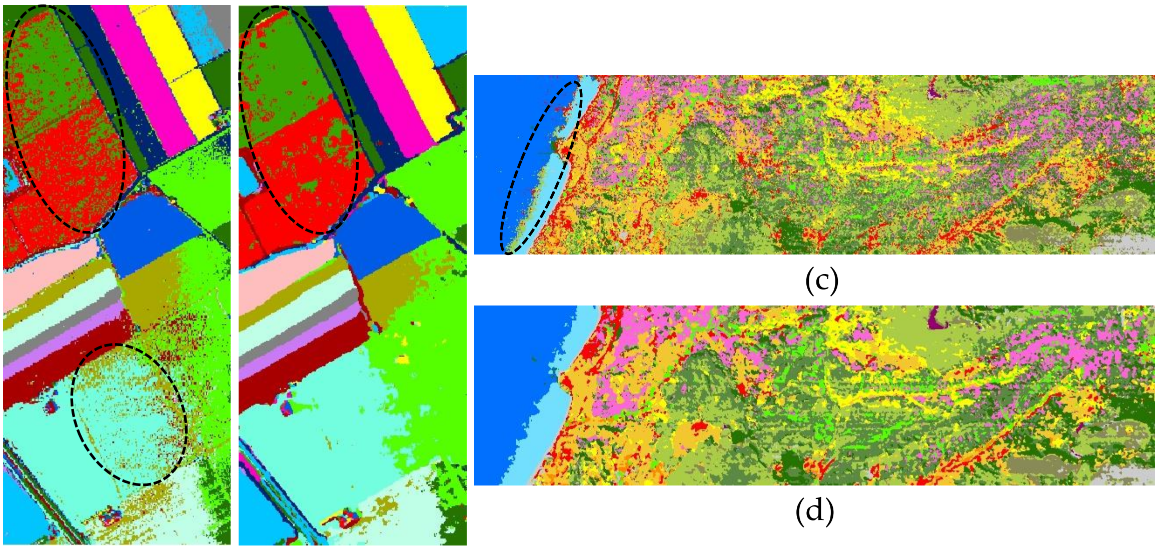

Figure 2. The classification maps for the SS dataset using (a) SVM and (b) CNN, and for the HL dataset using (c) SVM and (d) CNN respectively.

4. Conclusions

In this study, the classification of HSI datasets was evaluated with SVM and CNN algorithms. For this purpose, two publicly available datasets that include agricultural and forestry classes were evaluated. The experimental results given in Table 3 show that the CNN algorithm outperformed for both HSI data. For the SS data set, CNN showed a better performance by PA, UA and f scores against the SVM. For HL data set, CNN again gained better f scores in 10 of 14 land cover classes. Despite the high accuracy of the measured UA values, PA metrics were calculated very low in the Broad leaved forest and Coniferous forest classes. The reason of the low accuracy of HL could be the unbalanced ground truth data that was labeled without field studies and the low spatial resolution of the data provided by spaceborne sensor. However, the classification performance is sufficient despite the limited training data. Results showed that CNN models are useable on HSI classification problems that include agricultural and forestry areas.

Acknowledgments: The authors thank to the ISPRS Commission III, WG III/4 for providing the HyRANK dataset used in the experiments. This study was supported by Afyon Kocatepe University Scientific Research Projects Coordination Unit within the 20.FEN.BİL.12 project.

Conflicts of Interest: The authors declare no conflict of interest.

References

1. Dalponte, M., et al., The Role of Spectral Resolution and Classifier Complexity in the Analysis of Hyperspectral Images of Forest Areas. *Remote Sensing of Environment*, **2009**. 113(11): p. 2345-2355.
2. Gualtieri, J., et al. Support Vector Machine Classifiers as Applied to AVIRIS Data. in Proc. *Eighth JPL Airborne Geoscience Workshop*. **1999**. Pasadena.
3. Chan, J.C.-W. and D. Paelinckx, Evaluation of Random Forest and Adaboost Tree-based Ensemble Classification and Spectral Band Selection for Ecotope Mapping Using Airborne Hyperspectral Imagery. *Remote Sensing of Environment*, **2008**. 112(6): p. 2999-3011.
4. Luo, Y., et al. HSI-CNN: A Novel Convolution Neural Network for Hyperspectral Image. in 2018 International Conference on Audio, Language and Image Processing (ICALIP). 2018. Beijing: IEEE.
5. Roy, S.K., et al., HybridSN: Exploring 3-D–2-D CNN Feature Hierarchy for Hyperspectral Image Classification. *IEEE Geoscience and Remote Sensing Letters*, **2019**. 17(2): p. 277-281.
6. Cortes, C. and V. Vapnik, Support-Vector Networks. *Machine Learning*, **1995**. 20(3): p. 273-297.
7. Vapnik, V., *The Nature of Statistical Learning Theory*. 1995, New York: Springer - Verlag. 188.
8. Pal, M. and P. Mather, Support Vector Machines for Classification in Remote Sensing. *International Journal of Remote Sensing*, **2005**. 26(5): p. 1007-1011.
9. Christovam, L.E., et al., Land Use and Land Cover Classification Using Hyperspectral Imagery: Evaluating the Performance of Spectral Angle Mapper, Support Vector Machine and Random Forest, in International Archives of the Photogrammetry, Remote Sensing & Spatial Information Sciences. 2019: Enschede, The Netherlands. p. 1841-1847.
10. Tuia, D., et al., A survey of active learning algorithms for supervised remote sensing image classification. *IEEE Journal of Selected Topics in Signal Processing*, **2011**. 5(3): p. 606-617.
11. Kavzoglu, T. and I. Colkesen, A Kernel Functions Analysis for Support Vector Machines for Land Cover Classification. *International Journal of Applied Earth Observation and Geoinformation*, **2009**. 11(5): p. 352-359.
12. Mountrakis, G., J. Im, and C. Ogole, Support Vector Machines in Remote Sensing: A Review. *ISPRS Journal of Photogrammetry and Remote Sensing*, **2011**. 66(3): p. 247-259.
13. LeCun, Y., Y. Bengio, and G. Hinton, Deep Learning. *Nature*, **2015**. 521(7553): p. 436-444.
14. Guo, Y., et al., Deep Learning for Visual Understanding: A Review. *Neurocomputing*, **2016**. 187: p. 27-48.
15. Aloysius, N. and M. Geetha. A Review on Deep Convolutional Neural Networks. in 2017 International Conference on Communication and Signal Processing (ICCSP). 2017. Chennai, India: IEEE.
16. He, K., et al. Delving deep into rectifiers: Surpassing human-level performance on imagenet classification. in Proceedings of the IEEE international conference on computer vision. 2015.
17. Karantzalos, K., et al., HyRANK Hyperspectral Satellite Dataset I (Version v001), I.W. III/4, Editor. 2018.
18. Abadi, M., et al. Tensorflow: A system for large-scale machine learning. in 12th {USENIX} symposium on operating systems design and implementation ({OSDI} 16). 2016.
19. Pedregosa, F., et al., Scikit-learn: Machine learning in Python. *the Journal of machine Learning research*, **2011**. 12: p. 2825-2830.